AGU PUBLICATIONS

JGR

Journal of Geophysical Research: Biogeosciences

RESEARCH ARTICLE
10.1002/2017JG004180

Key Points:
- Sun-induced fluorescence was continuously measured at the canopy level across multiple growth stages in a soybean field
- The positive relationship between SIF and GPP was dominated by a strong relationship between SIF and APAR
- SIF yield was positively correlated with APAR and negatively correlated with LUE under stable sunny conditions

Supporting Information:
- Supporting Information S1
- Movie S1

Correspondence to:
G. Miao and K. Guan,
gmiao@illinois.edu;
kaiyug@illinois.edu

Citation:
Miao, G., Guan, K., Yang, X., Bernacchi, C. J., Berry, J. A., DeLucia, E. H., et al. (2018). Sun-induced chlorophyll fluorescence, photosynthesis, and light use efficiency of a soybean field from Seasonally Continuous Measurements. *Journal of Geophysical Research: Biogeosciences*, *123*, 610–623. https://doi.org/10.1002/2017JG004180

Received 22 SEP 2017
Accepted 21 JAN 2018
Accepted article online 29 JAN 2018
Published online 27 FEB 2018

Sun-Induced Chlorophyll Fluorescence, Photosynthesis, and Light Use Efficiency of a Soybean Field from Seasonally Continuous Measurements

Guofang Miao[1], Kaiyu Guan[1,2], Xi Yang[3], Carl J. Bernacchi[4,5,6], Joseph A. Berry[7], Evan H. DeLucia[4,6,8], Jin Wu[9], Caitlin E. Moore[4,6], Katherine Meacham[4,6], Yaping Cai[10], Bin Peng[2], Hyungsuk Kimm[1], and Michael D. Masters[4,6,8]

[1]Department of Natural Resources and Environmental Sciences, University of Illinois at Urbana-Champaign, Urbana, IL, USA, [2]National Center of Supercomputing Applications, University of Illinois at Urbana-Champaign, Urbana, IL, USA, [3]Department of Environmental Sciences, University of Virginia, Charlottesville, VA, USA, [4]Department of Plant Biology, University of Illinois at Urbana-Champaign, Urbana, IL, USA, [5]USDA ARS Global Change and Photosynthesis Research Unit, Urbana, IL, USA, [6]Carl R. Woese Institute for Genomic Biology, University of Illinois at Urbana-Champaign, Urbana, IL, USA, [7]Department of Global Ecology, Carnegie Institution for Science, Stanford, CA, USA, [8]Institute for Sustainability, Energy, and Environment, University of Illinois at Urbana-Champaign, Urbana, IL, USA, [9]Environmental and Climate Sciences Department, Brookhaven National Laboratory, Upton, NY, USA, [10]Department of Geography and Geographic Information Science, University of Illinois at Urbana-Champaign, Urbana, IL, USA

Abstract Recent development of sun-induced chlorophyll fluorescence (SIF) technology is stimulating studies to remotely approximate canopy photosynthesis (measured as gross primary production, GPP). While multiple applications have advanced the empirical relationship between GPP and SIF, mechanistic understanding of this relationship is still limited. GPP:SIF relationship, using the standard light use efficiency framework, is determined by absorbed photosynthetically active radiation (APAR) and the relationship between photosynthetic light use efficiency (LUE) and fluorescence yield (SIF_y). While previous studies have found that APAR is the dominant factor of the GPP:SIF relationship, the LUE:SIF_y relationship remains unclear. For a better understanding of the LUE:SIF_y relationship, we deployed a ground-based system (FluoSpec2), with an eddy-covariance flux tower at a soybean field in the Midwestern U.S. during the 2016 growing season to collect SIF and GPP data simultaneously. With the measurements categorized by plant growth stages, light conditions, and time scales, we confirmed that a strong positive GPP:SIF relationship was dominated by an even stronger linear SIF:APAR relationship. By normalizing both GPP and SIF by APAR, we found that under sunny conditions our soybean field exhibited a clear positive SIF_y:APAR relationship and a weak negative LUE:SIF_y relationship, opposite to the positive LUE:SIF_y relationship reported previously in other ecosystems. Our study provides a first continuous SIF record over multiple growth stages for agricultural systems and reveals a distinctive pattern related to the LUE:SIF_y relationship compared with previous work. The observed positive relationship of SIF_y:APAR at the soybean site provides new insights of the previous understanding on the SIF's physiological implications.

1. Introduction

During photosynthesis plants absorb sunlight in the 400–700 nm range of the electromagnetic spectrum, triggering the emission of light from leaves in the red and far-red (650–850 nm) known as sun-induced chlorophyll fluorescence (SIF) (Papageorgiou & Govindjee, 2004). The strong link between SIF and photosynthesis has opened up a new approach of approximating gross primary productivity (GPP), the gross uptake of atmospheric carbon dioxide (CO_2) through photosynthesis (Schlau-Cohen & Berry, 2015). Recent development of SIF technologies, including spaceborne (Frankenberg, Butz, et al., 2011; Guanter et al., 2014; Joiner et al., 2011, 2013), airborne (Damm et al., 2014; Rascher et al., 2015; Zarco-Tejada et al., 2009, 2012), and continuous ground-based techniques (Cogliati et al., 2015; Daumard et al., 2010; Drolet et al., 2014; Yang et al., 2015), have rapidly advanced the potential of SIF for monitoring terrestrial carbon uptake remotely across multiple temporal and spatial scales.

Previous studies have shown a quasi-linear GPP:SIF relationship in different ecosystems observed from diverse sources and across multiple spatial scales (Damm et al., 2015; Frankenberg, Fisher, et al., 2011;

Guanter et al., 2014; Perez-Priego et al., 2015; Verma et al., 2017; Wood et al., 2016; Yang et al., 2015). Multiple applications have taken this empirical relationship forward, for example, using SIF to infer GPP directly, constrain the estimate of photosynthesis capacity, or derive electron transport rate proportionally (Guan et al., 2016; Guanter et al., 2014; Perez-Priego et al., 2015; Zhang et al., 2014), but little justification has been made for the underlying processes associated with this relationship. The mechanistic understanding of the GPP:SIF relationship is still limited, which hampers further applications of SIF.

Photosynthesis, SIF, and heat dissipation are the three major pathways in which absorbed solar energy is utilized (Muller, 2001). Understanding the relationship between pathways relies on the partitioning of the absorbed light, that is, the fraction of absorbed photons going into each pathway. The partitioning of photosynthesis and SIF can be characterized by normalizing them with the absorbed light (Grace et al., 2007; Hilker et al., 2008), as expressed by Monteith's (1977) light use efficiency (LUE) model (equation (1)), in which APAR is the absorbed photosynthetically active radiation, and LUE and SIF_y are defined as photosynthetic LUE and SIF yield, respectively (Guanter et al., 2014). The relationship between LUE and SIF_y indicates how photosynthesis and SIF covary with each other.

$$\begin{cases} GPP = LUE \times APAR \\ SIF = SIF_y \times APAR \end{cases} \quad (1)$$

Equation (1) demonstrates that the GPP:SIF ratio is equal to the LUE:SIF_y ratio at instantaneous scales, but at a long-term scale, the GPP:SIF relationship is jointly determined by the variations in both APAR and the LUE:SIF_y relationship. However, due to the much larger variations in APAR than LUE and SIF_y, it has been found that APAR is generally the dominant factor that leads to the linear relationship between GPP and SIF (Rossini et al., 2010; Yang et al., 2015). Although previous studies also suggested that LUE and SIF_y contribute to the linear GPP:SIF relationship (Badgley et al., 2017), the remained variations in and the much smaller values of LUE and SIF_y implicitly determine the large uncertainties in the LUE:SIF_y relationship.

A prerequisite for improving our understanding of the LUE:SIF_y relationship is to determine the relationships of LUE and SIF_y with APAR, that is, the energy source. LUE and SIF_y also vary with change in APAR, which is affected by plant physiology (e.g., chlorophyll content and photosynthetic capacity) associated with stand age/plant growth stage, environmental conditions, and time scale (Gower et al., 1999; Hilker et al., 2008; Jenkins et al., 2007). At the canopy scale or beyond, canopy structure, which is related to ratio of sun to shaded leaves, leaf inclination angles, clumping, and the reabsorption of SIF etc, can play important roles on the observed SIF and consequently the SIF_y:APAR and LUE:SIF_y relationships (Fournier et al., 2012; Louis et al., 2005; Rascher et al., 2009). While the LUE:APAR relationship has been broadly investigated across various ecosystems (Turner et al., 2003), the SIF_y:APAR relationship is rarely reported and few types of ecosystems have been studied (Verma et al., 2017; Yang et al., 2015).

It has been observed that agricultural lands have remarkably high SIF (e.g., U.S. Corn Belt, Guanter et al., 2014) and SIF signal could be used as an indicator of vegetation stress status (Ac et al., 2015; Flexas et al., 2002; Perez-Priego et al., 2015, 2005), which is particularly valuable for monitoring crop productivity and stress (Guan et al., 2016). While there have been a few SIF studies on croplands, most of them are based on spaceborne and airborne sensors covering sporadic sunny days (Alexander Damm et al., 2010; Damm et al., 2015; Liu et al., 2017; Pinto et al., 2016; Zarco-Tejada et al., 2013). Ground-based continuous techniques have the advantage of covering all light conditions and capturing both short- and long-term variations, with much less noise from atmospheric effects due to the close distance between plants and sensors (Frankenberg, Butz, et al., 2011; Malenovsky et al., 2009; Meroni et al., 2009). This could help to disentangle the confounding effects associated with environmental stresses, plant growth stages, or time scales on LUE, SIF_y, and the relationship between them. We deployed an automated ground-based SIF system at a soybean field in the Midwestern USA, paired with an existing eddy-covariance (EC) flux tower, to continuously collect optical signals for SIF retrieval in 2016 growing season. The major objectives of this study were to investigate (1) the GPP:SIF relationships at diurnal and seasonal scales, (2) the SIF_y:APAR and LUE:APAR relationships, and (3) the relationship between SIF_y and LUE at multiple temporal scales and under different light conditions.

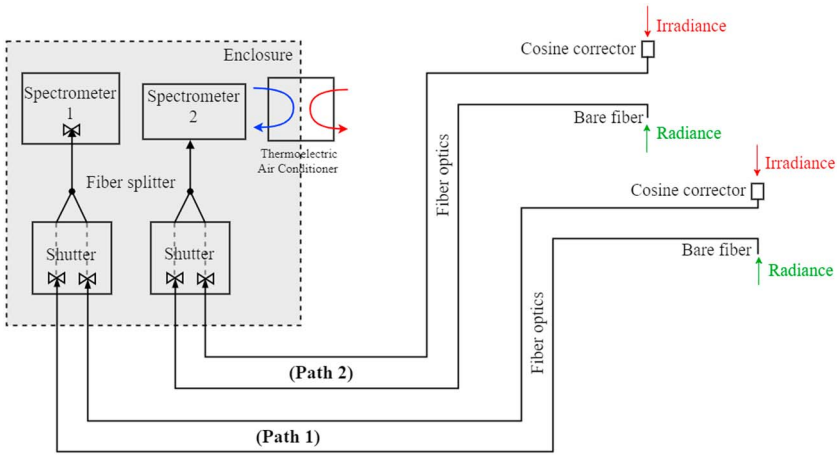

Figure 1. Schematic diagram of a Fluospec2 system.

2. Materials and Methods

2.1. Site Description

The study site is located at the Energy Farm of the University of Illinois at Urbana-Champaign, USA (40.065791 N, 88.208387 W, and ~220 m elevation). The mean annual air temperature and total precipitation from climate records of an adjacent station (Champaign, Illinois State Water Survey) are 11.1 °C and 1048 mm, respectively, for the period of 1981–2010. The average air temperature of growing season (from April to September) is 19.4 °C, and precipitation is 625 mm. In 2016, the mean annual air temperature and precipitation were 12.5 °C and 1025 mm, respectively. The average growing season air temperature was 20.2 °C, and precipitation was 715 mm.

The soybean (*Glycine max* L.) plot, 200 m × 200 m, is a long-term EC flux site with a maize/maize/soybean rotation since 2008 (Joo et al., 2016; Zeri et al., 2011). The sowing date for 2016 was 26 May, and the study was conducted from 11 August to 20 September, covering the soybean reproductive stages from R3 (beginning pod) to R7 (beginning maturity) (Fehr et al., 1971). The leaf area index was 6.6 ± 0.3 at the beginning of the study and was 2.0 ± 0.1 at the end.

2.2. Field Instrumentation: FluoSpec2 System and Eddy-Covariance Flux System

We installed the FluoSpec2 system (Yang et al., 2015, Figure 1; field images in Figure S1 in the supporting information) in the field to collect signals required for SIF retrieval and several associated vegetation indices. The FluoSpec2 system included two spectrometers: one (Path 1) covered wavelength from 730 to 780 nm with an optical resolution of 0.15 nm (measured as full width half maximum, QEPRO embedded with an internal shutter, Ocean Optics, Dunedin, FL, USA), which is specifically for SIF retrievals at the O_2-A band. The other (Path 2) covered wavelength of 350–1100 nm with the optical resolution of 1.10 nm (HR2000+, Ocean Optics), which served as a spectrometer that can provide canopy reflectance and standard vegetation indices. Each path contained two optical fibers, with one collecting optical signals from the sun (irradiance) and the other collecting signals from the crop canopy (radiance). One inline shutter switches between irradiance and radiance for one spectrometer. The irradiance fiber was attached with a cosine corrector to have a field of view of 180°, while the radiance fiber had a 25° field of view. The irradiance signal was directly calibrated with a standard light source (HL-CAL-2000, Ocean Optics), and the radiance signal was calibrated through a standard reflection board (Spectralon®, Labsphere, NH, USA) at noontime. Field calibration was conducted for the system before and after the field data collection to estimate the potential signal drift. The inline shutters and spectrometers were installed in a temperature-controlled enclosure for field measurement (Figure 1). Specific configuration of each path was described in Table S1 in the supporting information.

An EC flux system including meteorological sensors was installed in parallel to measure the above-canopy gas exchange. The EC system consisted of a 3-D sonic anemometer (81000VRE, R.M. Young, Traverse City, MI, USA) and an open-path infrared gas analyzer (LI-7500, LI-COR, Lincoln, NE, USA). Meteorological variables measured above the canopy included air temperature and relative humidity (HMP-45C, Campbell Scientific,

Logan, UT, USA), upwelling and downwelling photosynthetic photon flux density (LI-190, LI-COR, Lincoln, NE, USA) and short- and long-wave radiation (CNR1, Delft, Kipp & Zonen, Netherlands). All above-canopy sensors were mounted at 4 m. The ground auxiliary measurements included soil temperature and soil moisture (Hydra Probe II, Stevens Water Monitoring Systems, OR, USA) at four levels (10, 20, 50, and 75 cm below ground) and soil heat flux (HFP01, Hukseflux Thermal Sensors B.V., Delft, Netherlands) at 10 cm below ground.

Ecosystem fluxes were calculated following procedures and configurations from previous studies conducted at the same site (Joo et al., 2016; Zeri et al., 2011). The 10 Hz raw data were first processed using EddyPro software (version 6.1.0, LI-COR, Lincoln, NE, USA) for coordinate alignment (double rotation method), compensation of density fluctuations (Webb et al., 1980), low- and high-frequency spectral corrections (Moncrieff et al., 1997, 2004), and calculating turbulent flux and CO_2 storage flux. The turbulent flux integrated with the CO_2 storage change is referred to the net ecosystem CO_2 exchange. Further data quality control and net ecosystem CO_2 exchange separation to GPP and ecosystem respiration followed the standard procedure from Papale et al. (2006) and Reichstein et al. (2005).

2.3. SIF Retrieval and Vegetation Indices

Sun-induced chlorophyll fluorescence was calculated using the spectral fitting method (Meroni et al., 2009; Yang et al., 2015). The basic assumption of the spectral fitting method (equation (2)) is that upwelling radiance (L) from a canopy is composed of a reflected signal (reflectance [r, dimensionless] × irradiance [E, m W m^{-2} nm^{-1} sr^{-1}]) and an emitted one (F, m W m^{-2} nm^{-1} sr^{-1}), in which L and E could be directly measured. The emitted fluorescence and reflectance are assumed linearly related with the wavelength (λ) at the selected band, and the coefficients (a, b, c, and d) are derived from the regression between L, E, and λ as in equation (2). SIF is then calculated as the regression response at the wavelength of 760 nm (equation (3)). The irradiance and radiance measured by Path 1 of the FluoSpec2 system at 1 min interval were applied for SIF retrieval. The 1 min retrieved SIF was averaged every 30 min to match with the frequency and timestamp of EC flux data.

$$L = \frac{rE}{\pi} + F \cong \frac{(a + b\lambda)E}{\pi} + (c + d\lambda), \lambda \in (759.00, 767.76\ \text{nm}) \tag{2}$$

$$\text{SIF} = F_{760} = c + d \times 760 \tag{3}$$

Two vegetation indices were derived from the reflectance collected by Path 2 of the FluoSpec2 system as proxies to track phenological and physiological changes. Specifically, the Normalized Difference Vegetation Index (NDVI $= \frac{r_{770-780} - r_{650-660}}{r_{770-780} + r_{650-660}}$, Tucker, 1979), a proxy of canopy structure, and Rededge Index (Rededge $= \frac{r_{750}}{r_{705}}$, Gitelson & Merzlyakb, 1994), a proxy of canopy chlorophyll content, were paired to identify the growth stages. The Rededge NDVI (Rededge_NDVI $= \frac{r_{750} - r_{705}}{r_{750} + r_{705}}$, Viña & Gitelson, 2005) was used to approximate the fraction of APAR (fAPAR) in PAR (section 2.4).

2.4. Data Processing and Analysis for Different Temporal Scales and Light Conditions

With SIF, GPP, and PAR data, the LUE model (equation (1)) was applied to derive LUE and SIF_y. Since we did not directly measure APAR, we calculated it as the product of PAR and $fAPAR_{green}$, in which $fAPAR_{green}$ refers to the fAPAR that has been absorbed by green leaves (i.e., photosynthetically active leaves). We used the Rededge_NDVI as the proxy of $fAPAR_{green}$ (equation (4)). Rededge_NDVI was proposed by Viña and Gitelson (2005) for studying soybean and maize in Nebraska and was found to be the best index for $fAPAR_{green}$ among various other vegetation indices. It is worth noting that we also used other vegetation indices, for example, green NDVI (green_NDVI $= \frac{r_{770-780} - r_{550-560}}{r_{77-780} + r_{550-560}}$, Viña & Gitelson, 2005) and MERIS Terrestrial Chlorophyll Index (MTCI $= \frac{r_{770-780} - r_{704-714}}{r_{704-714} - r_{650-660}}$, Viña et al., 2011) to approximate $fAPAR_{green}$ (Figures S3 and S4) and found that different formulated $fAPAR_{green}$ had little impacts on the general pattern of our results shown in section 3.

$$\begin{cases} APAR = PAR \times fAPAR_{green} \\ fAPAR_{green} = 1.37 \times \text{Rededge\_NDVI} - 0.17 \end{cases} \tag{4}$$

In addition to the analysis of apparent plant response reflected by GPP:SIF, SIF:APAR, and GPP:APAR relationships, we further explored the SIF_y:APAR and LUE:APAR relationships through the intrinsic response of individual pathways to light conditions. Last, the LUE:SIF_y relationship was discussed for a direct comparison between the two pathways.

To disentangle the effects of different plant growth stages on the plant response to environmental conditions, we categorized the whole 30 min data set following the workflow shown in Figure S2. Plants did not experience significant water/heat stress across the study period; therefore, the environmental changes only referred to the variation in light conditions in this current study. At every category, GPP:SIF and the relationships of the other associated variables (mainly referring to the relationships of SIF:APAR, GPP:APAR, SIF_y:APAR, LUE:APAR, and LUE:SIF_y hereafter) were analyzed accordingly.

Growth phases were first identified from the time series of NDVI (the proxy of phenology) and Rededge (the proxy of chlorophyll content) indices. The rationale of using the paired indices to divide the growth phases is that we define periods during which the effects of individual factors impacting GPP, SIF, and APAR can be possibly distinguished from each other. For example, if both NDVI and Rededge are constant at one phase, then the relationship of SIF, SIF_y, or GPP and LUE with APAR implies the true response of plants to absorbed energy at this specific phase.

Second, we defined a sunlight threshold by comparing the actual PAR with theoretical PAR to distinguish sunny and cloudy conditions. Theoretical PAR was derived from dates and solar zenith angle of every 30 min (Weiss & Norman, 1985). We calculated the ratio of actual PAR to theoretical PAR and set the ratio threshold of 0.6. It was defined as sunny when a ratio was greater than 0.6 and as cloudy otherwise. This threshold was applied for all the time scales discussed in this study.

Diurnal variation of the GPP:SIF relationship and the relationships of other paired variables was then investigated for individual growth phases, by which the effect of growth phases can be excluded largely. Furthermore, sunny days and cloudy days were separated at every phase, and diurnal pattern of all the relationships was analyzed under each light condition.

Seasonal changes of GPP:SIF and other variables' relationships were investigated across multiple phases with the diurnal variations removed by averaging daily data. Meanwhile, due to the rapid change of light conditions at diurnal scale (especially during cloudy days) and that GPP, SIF, and associated variables may respond to light differently, impetuous averaging a whole day data would conceal the actual differences between days and between phases. To minimize this averaging uncertainty while also reducing the influence from short-term fluctuation, we examined the data and found that, during this study period, the weather appeared mostly cloudy in the morning and sunny in the afternoon. Therefore, we averaged the data by morning (9–12), midday (12–14), and afternoon (14–17) every day instead of the daily mean of 9–17.

Overall, during the 41 day study period, there were 30 (73%) days of data involved in this study, of which 17 (57%) were sunny days and 13 (43%) cloudy or partly cloudy days. Days when precipitation events occurred during the daytime were excluded.

3. Results

3.1. Growth Phases Identified by Vegetation Indices

Daily mean SIF and GPP decreased continuously during the study period (11 August to 20 September) at the soybean site (Figure 2a), with a seasonal variation of 1.7 ± 0.5 (mean ± SD) mW m^{-2} nm^{-1} sr^{-1} in SIF and 28.7 ± 6.8 μmol C m^{-2} s^{-1} in GPP. Based on seasonal trajectories of NDVI and Rededge, we distinguished three phenological/physiological phases (Figure 2b): Phase 1, 11–31 August 2016 (21 days), during which both NDVI and Rededge were in their peak period and a relatively stable status; Phase 2, 1–7 September 2016 (7 days), during which NDVI was stable while Rededge was decreasing; and Phase 3, 8–20 September 2016 (13 days), during which both NDVI and Rededge decreased rapidly. The absolute cut-off day for each stage was uncertain, but 1–2 day shift did not affect the results. The following relationship analysis mainly focused on the first two phases when photosynthesis was still active.

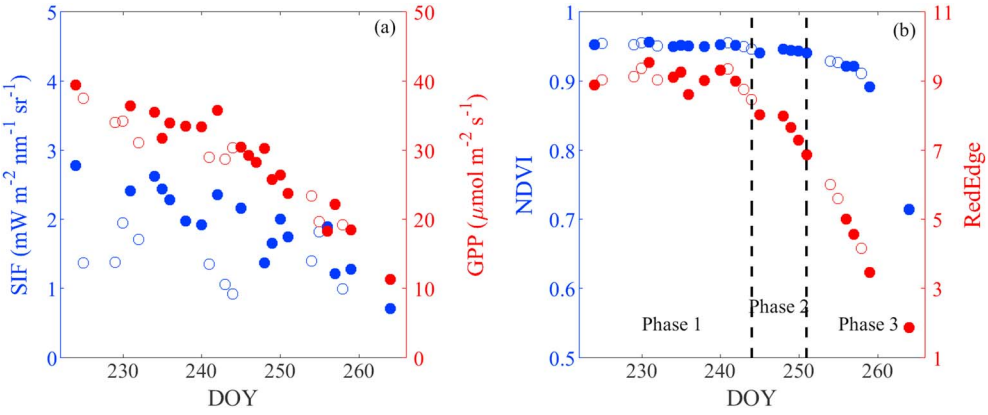

Figure 2. Daily mean time series at the soybean field from 11 August to 20 September (day of year 224 to 264): (a) Sun-induced chlorophyll fluorescence (SIF) and gross primary productivity (GPP) and (b) Normalized Difference Vegetation Index (NDVI) and Rededge Index. The solid circles represent for sunny days and open circles for cloudy days.

3.2. Overall GPP:SIF and LUE:SIF$_y$ Relationships

The whole 30 min data exhibited strong positive GPP:SIF relationship ($R^2 = 0.46$, $p < 0.01$, Figure 3a). SIF was highly correlated with APAR positively ($R^2 = 0.83$, $p < 0.01$, Figure 3b), while GPP was also positively correlated with APAR but with a lower R^2 ($R^2 = 0.52$, $p < 0.01$, Figure 3c).

After SIF and GPP were normalized by APAR, SIF$_y$ and LUE were weakly correlated with APAR. SIF$_y$ and APAR were positively correlated ($R^2 = 0.28$, $p < 0.01$, Figure 3d), and LUE and APAR were negatively correlated ($R^2 = 0.38$, $p < 0.01$, Figure 3e) with a concave shape as has been reported previously (Damm et al., 2015; Liu et al., 2017). SIF$_y$ and LUE had a weak negative correlation ($R^2 = 0.067$, Figure 3f and Table S3), though it was statistically significant ($p < 0.01$).

3.3. GPP:SIF and LUE:SIF$_y$ Relationships at the Diurnal Scale

Local light condition during the study period changed rapidly at the diurnal scale, especially from noontime to late afternoon. Even for the cloudy days defined by the sunlight threshold, most of the days had occasional sunny moments (e.g., the black line in Figure 4b). GPP and SIF responded simultaneously to these light condition changes. The diurnal SIF and GPP variations were comparable to and even larger than the seasonal variations. The SIF variation was 2.3 ± 1.0 (mean ± SD) mW m^{-2} nm^{-1} sr^{-1} on a typical sunny day and 1.7 ± 0.8 mW m^{-2} nm^{-1} sr^{-1} on a cloudy day. Likewise, GPP was 34.0 ± 9.6 μmol C m^{-2} s^{-1} on a sunny day and 31.1 ± 9.8 μmol C m^{-2} s^{-1} on a cloudy day (Figure 4).

Generally, all the diurnal scale relationships between the six paired variables (i.e., GPP:SIF, SIF:APAR, GPP:APAR, SIF$_y$:APAR, LUE:APAR, and LUE:SIF$_y$) were consistent between sunny and cloudy days (Figures 5 and 6). Since Phases 1 and 2 did not exhibit significant differences in these relationships (results not shown here), here we only presented the results from Phase 1. The diurnal scale relationships were consistent with those from the whole 30 min data (Figure 3). Despite the consistency, at the diurnal scale, GPP and SIF had a stronger linear relationship on sunny days ($R^2 = 0.65$, $p < 0.01$, Figure 5a) than on cloudy days ($R^2 = 0.52$, $p < 0.01$, Figure 6a). SIF:APAR (Figures 5b and 6b) and GPP:APAR (Figures 5c and 6c) relationships both had a good linear pattern at the diurnal scale.

The LUE- and SIF$_y$-related relationships showed large differences between the two light conditions. The SIF$_y$:APAR relationship had larger R^2 on sunny days ($R^2 = 0.43$, $p < 0.01$, Figure 5d) than on cloudy days ($R^2 = 0.12$, $p < 0.01$, Figure 6d), though both were significant. In contrast, the LUE:APAR relationship had larger R^2 on cloudy days ($R^2 = 0.52$, $p < 0.01$, Figure 5e) and a steeper regression slope (Table S3) than on sunny days ($R^2 = 0.33$, $p < 0.01$, Figure 6e). These significant differences were primarily caused not only by the data in the cloudy mornings but also by the more unstable light condition during cloudy days (Figure 5d versus Figure 6d). Both SIF$_y$ and LUE at the diurnal scale were high under the low APAR, although the trend in SIF$_y$ (Figure 6d) was not as clear as in LUE

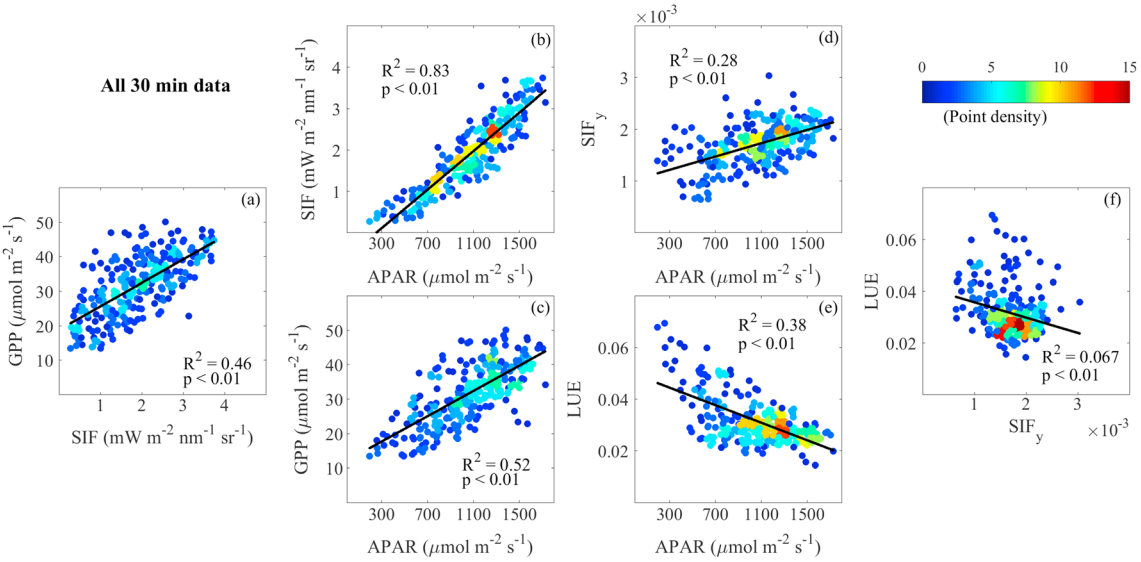

Figure 3. Relationships based on all 30 min data: (a) gross primary productivity (GPP):Sun-induced chlorophyll fluorescence (SIF), (b) SIF:absorbed photosynthetically active radiation (APAR), (c) Sun-induced chlorophyll fluorescence yield (SIF_y):APAR, (d) GPP:APAR, (e) light use efficiency (LUE):APAR, and (f) LUE:SIF_y over the study period at the soybean site. The color scheme represents point density. A linear regression between the paired variables is applied when such a relationship is statistically significant ($p < 0.01$).

(Figure 6e). LUE and SIF_y were negatively correlated on both sunny (R^2 = 0.069, $p < 0.01$, Figure 5f) and cloudy days (R^2 = 0.017, p = 0.23, Figure 6f), though this correlation was weak.

3.4. GPP:SIF and LUE:SIF_y Relationships at Seasonal Scale

The GPP:SIF, SIF:APAR, and GPP:APAR relationships were weaker at the seasonal scale than at the diurnal scale (Figures 7a–7c), partly due to the greater variation in light condition between days. The SIF_y:APAR and LUE:SIF_y relationships between sunny and cloudy conditions exhibited clearer differences at the seasonal scale (Figures 7d and 7f) than at the diurnal scale. SIF_y was negatively correlated with APAR under cloudy conditions despite the lack of statistical significance (R^2 = 0.36, p = 0.21, Figure 7d and Table S3), but they were positively correlated under sunny conditions and statistically significant (R^2 = 0.33, p = 0.02). If we fit the cloudy and sunny data together with a quadratic equation, a turning point of APAR that reaches the lowest SIF_y existed at approximately 840 μmol m^{-2} s^{-1} (p = 0.03). In contrast, LUE:APAR was consistently negative under both sunny and cloudy conditions (R^2 = 0.76, $p < 0.01$, Figure 7e). Accordingly, LUE and SIF_y were positively correlated under cloudy

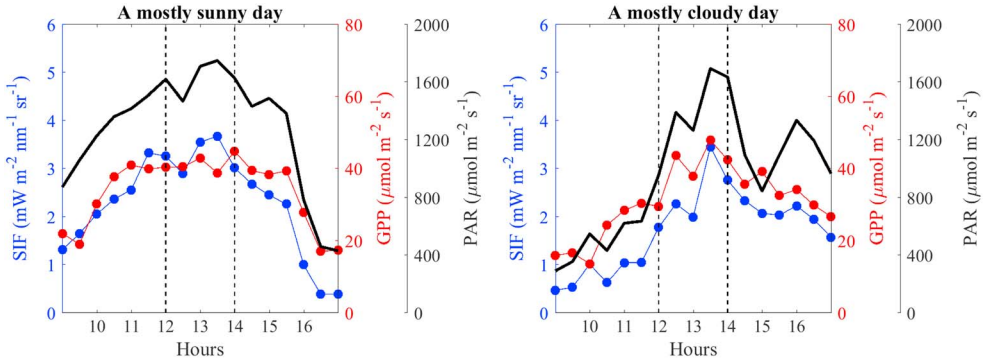

Figure 4. Examples of the diurnal cycles of sun-induced chlorophyll fluorescence (SIF), gross primary productivity (GPP), and photosynthetically active radiation (PAR) at (a) a mostly sunny day and (b) a mostly cloudy day. The dashed line marks the separation of the whole day data to morning (9–12), noontime (12–14), and afternoon (14–17).

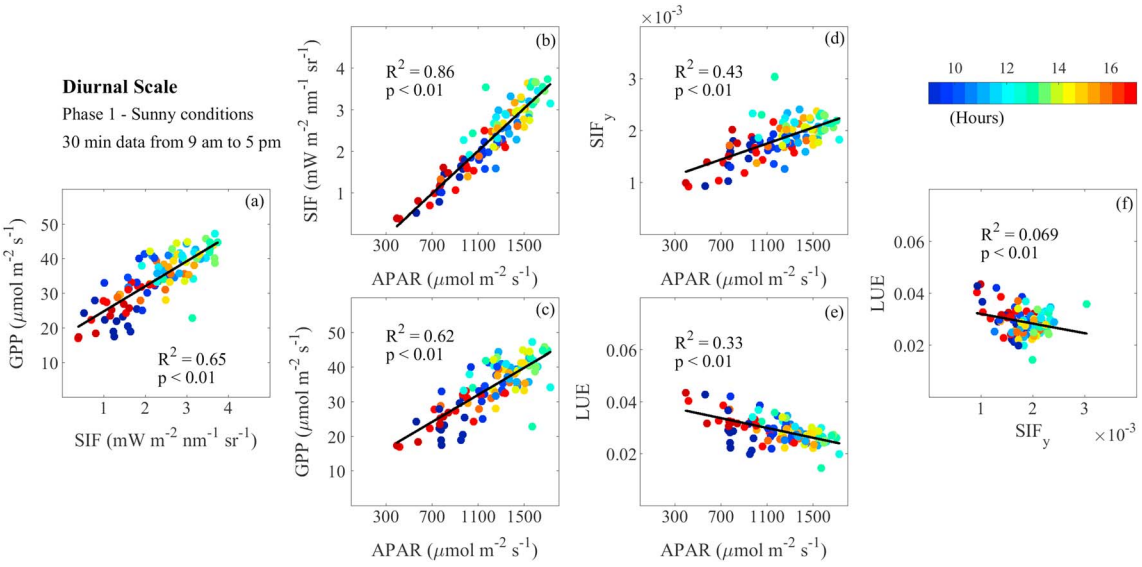

Figure 5. Relationships based on the 30 min data at the soybean field under sunny conditions at Phase 1 (both canopy structure and physiological status were relatively stable): (a) gross primary productivity (GPP):Sun-induced chlorophyll fluorescence (SIF), (b) SIF:absorbed photosynthetically active radiation (APAR), (c) GPP:APAR, (d) Sun-induced chlorophyll fluorescence yield (SIF_y):APAR, (e) light use efficiency (LUE):APAR, and (f) LUE:SIF_y. The color scheme represents the time stamps at 30 min interval from 9 to 17. A linear regression between the paired variables is applied when such a relationship is statistically significant ($p < 0.01$).

conditions (R^2 = 0.70, p = 0.039, Figure 7f). There was no clear pattern in the LUE:SIF_y relationship under sunny conditions at the seasonal scale (p = 0.41).

Both GPP and LUE had lower values in Phases 2 than 1, which did not occur in SIF and SIF_y (Figures 7a–7c). Due to the very short period of Phase 2, it was difficult to separate cloudy and sunny conditions for a meaningful comparison in this current study. Further investigation is required to determine whether GPP, SIF, and especially the corresponding LUE and SIF_y would exhibit different patterns under cloudy conditions at this transition phase from active growth to senescence stage.

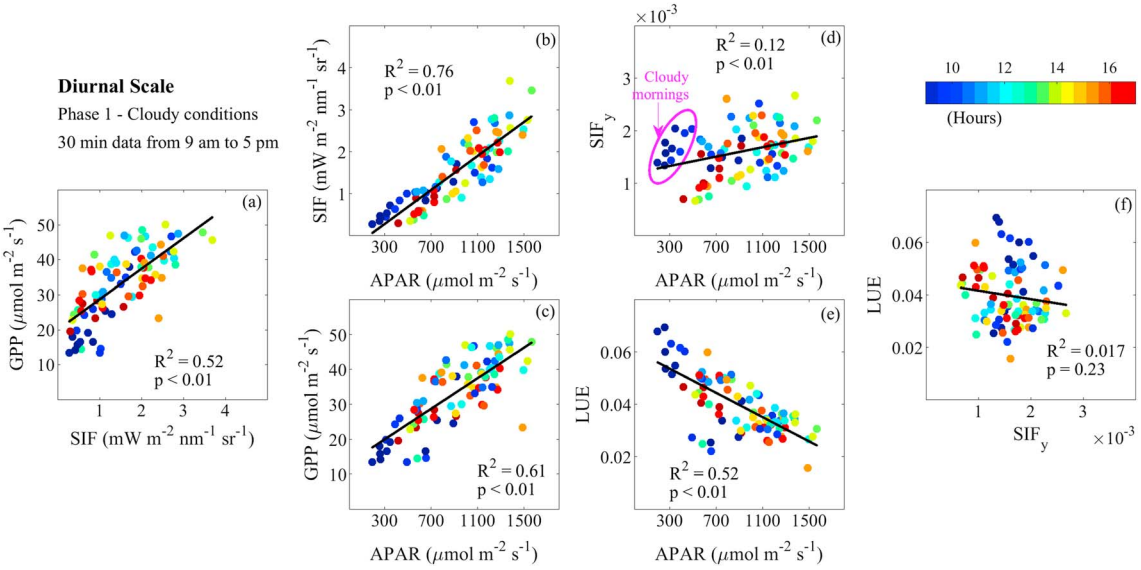

Figure 6. Relationships based on the 30 min data at the soybean field under cloudy conditions at Phase 1 (11–31 August, both canopy structure and physiological status were relatively stable): (a) gross primary productivity (GPP):Sun-induced chlorophyll fluorescence (SIF), (b) SIF:absorbed photosynthetically active radiation (APAR), (c) GPP:APAR, (d) Sun-induced chlorophyll fluorescence yield (SIF_y):APAR with the cloudy morning measurements highlighted, (e) light use efficiency (LUE):APAR, and (f) LUE:SIF_y. The color scheme represents the time stamps at 30 min interval from 9 to 17. A linear regression between the paired variables is applied when such a relationship is statistically significant ($p < 0.01$).

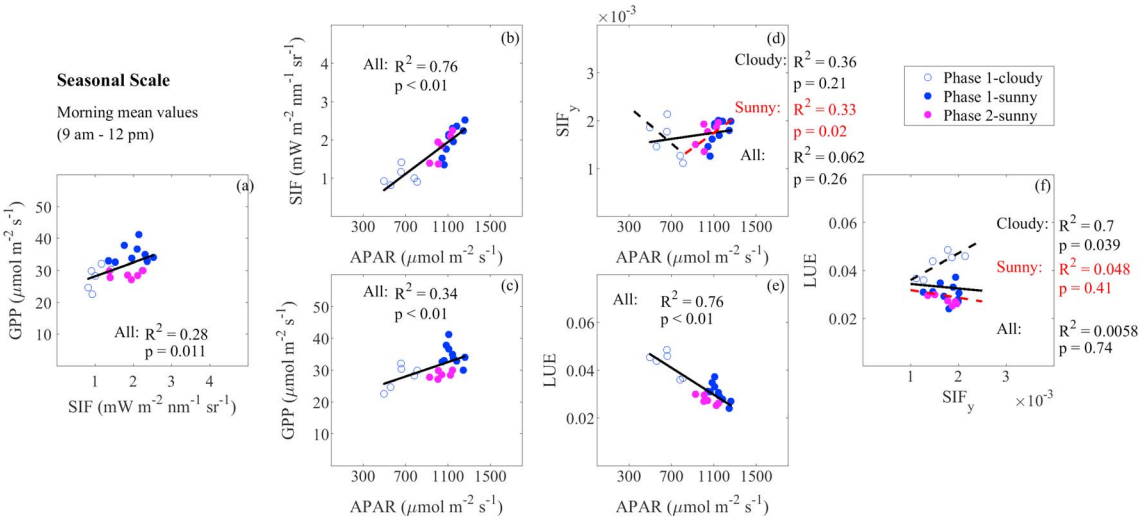

Figure 7. Relationships at the seasonal scale covering Phases 1 and 2 at the soybean field: (a) gross primary productivity (GPP):Sun-induced chlorophyll fluorescence (SIF), (b) SIF:absorbed photosynthetically active radiation (APAR), (c) Sun-induced chlorophyll fluorescence yield (SIF_y):APAR, (d) GPP:APAR, (e) light use efficiency (LUE):APAR, and (f) LUE:SIF_y. Data presented are mean values from 9 to 12 of every day. A linear regression between the paired variables is applied when such a relationship is statistically significant ($p < 0.01$). When $p > 0.01$, further regression fit is applied to sunny and cloudy conditions separately. See Figures S5 and S6 for data from 12 to 14 and from 14 to 17 of every day.

4. Discussion

Mechanistic understanding on the spatiotemporal variability of SIF and the SIF:GPP relationship is still in its early stage. By deploying a ground-based spectral system to collect SIF signals continuously, we were able to capture the SIF and SIF_y variations under different light conditions and over multiple growth phases at a soybean field in the Midwestern USA. Through the framework of categorizing the continuous measurements by growth phases, light conditions, and time scales (Figure S2), we disentangled the confounding effects from growth stages, light conditions, and time scales on GPP:SIF and other associated relationships. To our best knowledge, our study represents the first agricultural based continuous SIF measurements over multiple growth stages and paired with the EC flux measures. These data also provide the valuable validation resources for modeling studies (Van Der Tol et al., 2016; Zhang et al., 2016).

4.1. Comparison Between Soybean and Other Terrestrial Ecosystems

Overall, the general GPP:SIF, SIF:APAR, and GPP:APAR relationships observed at both diurnal and seasonal scales at the soybean field were consistent with previous observations measured at other ecosystems (Alexander Damm et al., 2010; Damm et al., 2015; Yang et al., 2015; Zarco-Tejada et al., 2013). GPP was more linearly correlated with SIF during sunny days when light condition was stable, while the GPP:SIF relationship showed an asymptotic trend during cloudy days with light condition changing rapidly. The highly correlated and positive relationship between SIF and APAR confirmed that the majority of the GPP:SIF relationship could be attributed to the fact that SIF carries much APAR information (Rossini et al., 2010; Yang et al., 2015). When GPP and SIF were normalized by APAR, however, SIF_y and LUE showed different relationships with APAR. Specifically, LUE was negatively correlated with APAR, while SIF_y was positively correlated with APAR at our site.

Our results of the SIF_y:APAR and LUE:SIF_y relationships at the soybean field showed some convergence but also inconsistent patterns with previous SIF studies (Table 1). At the diurnal scale, Damm et al. (2010) also observed negative LUE:SIF_y relationship at corn fields, which is consistent with our finding at the diurnal scale. At the seasonal scale, we compared our results with previous results reported for temperate forests (Yang et al., 2015) and a C4 grassland (Verma et al., 2017). Under cloudy conditions, our soybean field showed a weak positive LUE:SIF_y relationship (derived from the relationship that both LUE and SIF_y were negatively correlated with APAR, Figure 8). This weak positive LUE:SIF_y relationship was also found in the long-term SIF measurements conducted at the Harvard Forest site (Yang et al., 2015). In contrast, though Verma et al. (2017) also reported a positive LUE:SIF_y relationship in an Australian C4 grassland, they found that both LUE and SIF_y were positively correlated with APAR. Under sunny conditions, our study observed negative

Table 1
Comparison of the LUE:APAR, SIF_y:APAR, and LUE:SIF_y Relationships Between Different Ecosystems

	LUE:APAR	SIF_y:APAR	LUE:SIF_y	Data sources	References
Diurnal scale					
Soybean (sunny)	Negative	Positive	Negative	Ground	This study
Corn			Negative	Ground	Damm et al. (2010)
Seasonal scale					
Soybean (cloudy)	Negative	Negative	Weak positive	Ground	This study
Soybean (sunny)	Negative	Positive	Negative	Ground	This study
Temperate forest	Negative	Negative	Positive	Ground	Yang et al. (2015)
C_4 Grassland	Positive	Positive	Positive	Satellite	Verma et al. (2017)
Diurnal and extrapolated seasonal scales					
Soybean and deciduous broadleaf forest (low light)	Negative	Positive	Negative	SCOPE model	Zhang et al. (2016)
Soybean and deciduous broadleaf forest (high light)[a]	Negative	Negative	Positive	SCOPE model	Zhang et al. (2016)

Note. LUE, light use efficiency; SIF_y, Sun-induced chlorophyll fluorescence yield; APAR, absorbed photosynthetically active radiation; SCOPE, Soil-Canopy Observation Photosynthesis and Energy fluxes.
[a]The high light condition defined in the modeling study is similar to the sunny conditions in our study.

LUE:APAR and positive SIF_y:APAR relationships (Figure 8), resulting in a negative LUE:SIF_y relationship, contrary to both prior studies (Verma et al., 2017; Yang et al., 2015). These patterns derived from observations at the canopy scale or larger also differed from previous modeled results. Specifically, modeling results from the widely used Soil-Canopy Observation Photosynthesis and Energy (SCOPE) fluxes model suggested the general pattern for different types of ecosystems (e.g., C3 crops and deciduous broadleaf forests); that is, under low light conditions, the simulated LUE is negatively correlated with SIF_y, while under high light conditions, LUE and SIF_y are positively correlated (Flexas et al., 2002; Porcar-Castell et al., 2014; Van Der Tol et al., 2009), but the dominant pattern simulated was the positive LUE:SIF_y relationship (Zhang et al., 2016).

4.2. Physiological and Structural Controls on the Canopy-Level LUE:SIF_y Relationship

Both positive and negative LUE:SIF_y and SIF_y:APAR relationships can be possible as a result of energy partitioning due to various light and plant stress conditions. Schlau-Cohen and Berry (2015) discussed the theory of plant photosynthetic regulatory systems at the leaf level and the consequent light partitioning based on previous leaf light-response experiments (Demmig & Björkman, 1987), and they suggested that plants under varying conditions (e.g., limited, saturated light conditions, or drought) could show different coupling patterns between LUE and SIF_y. Generally, LUE decreases with the APAR increase, although the decreasing rate varies with the light intensity. SIF_y, however, could exhibit opposite patterns—when light is limiting, SIF_y increases with the APAR increase; when light becomes rate saturating or plants experience stress, SIF_y starts

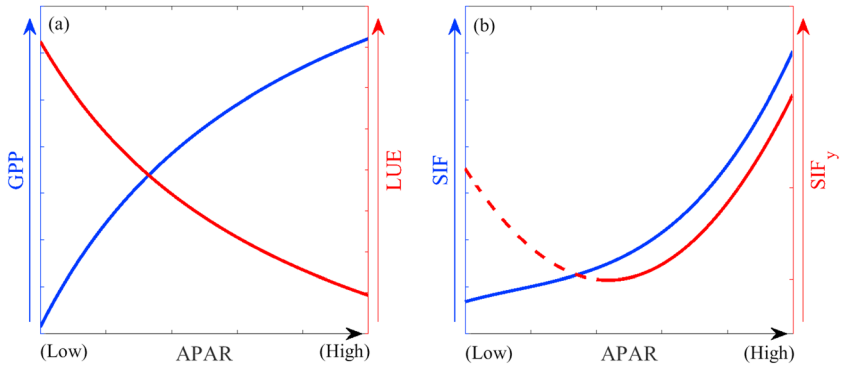

Figure 8. Generalized pattern from our results: (a) gross primary productivity (GPP):absorbed photosynthetically active radiation (APAR) and light use efficiency (LUE):APAR relationships, and (b) Sun-induced chlorophyll fluorescence (SIF): APAR, and Sun-induced chlorophyll fluorescence yield (SIF_y):APAR relationships. The arrows indicate values from low to high. The red dashed line represents cloudy conditions (different from the low light sunny conditions).

decreasing as well. As a result, LUE:SIF_y relationship could be positive under light-saturating conditions while negative under light-limiting condition (Van Der Tol et al., 2014). This trend is potentially applicable to various ecosystems, but the threshold of light-limiting/light-saturating may depend on species, ecosystem, or specific site. When we consider the canopy level, the variation of light or stress conditions may differ for individual leaves, which could be also site or ecosystem specific (Pearcy, 1990). The integrated responses of individual leaves over the whole canopy result in the canopy-level LUE:SIF_y relationship.

Soybean, a C3 species with high photosynthetic capacity, if there is no severe stress, usually exhibits slightly light-saturated or nonsaturated photosynthesis at the canopy level (Gitelson et al., 2015; Slattery et al., 2017; Suyker et al., 2005). Our soybean field did not experience obvious stresses during the study period; thus, the coupling between photosynthesis and SIF may be largely driven by light condition. The characteristics of light nonsaturated or slightly saturated photosynthesis may result in the positive SIF_y:APAR and the negative LUE:SIF_y relationship that we observed during sunny days even though the significance of the latter was weak. Specifically, it is likely that at our soybean field some leaves that were deeply shaded (high LUE, low SIF_y due to the limited light, Schlau-Cohen & Berry, 2015) in the early morning or late afternoon became exposed to the sun (lower LUE, higher SIF_y with the increasing APAR) in the midday. Early studies also observed that light penetrates deep at high solar elevations (Lemeur, 1973). The responses of shaded leaves to the variations of the light condition in the canopy could be attributed to the positive SIF_y:APAR and negative LUE:SIF_y relationships, which is consistent with the finding in Schlau-Cohen and Berry (2015) and Demmig and Björkman (1987) for the changes from deep shaded to sunlit conditions. Similar scenarios of light condition variations could occur at the seasonal scale, in which the exposure of leaves to the sun or photosynthetic capacity of leaves varied with the change of light conditions. In addition, soybean has specific strategies of reorientating leaves in response to the direction and intensity of sunlight (see the leaf movement video in the supporting information), and the orientation strategies differ under cloudy and sunny conditions (Koller, 1990). This might also explain our observed patterns in SIF_y:APAR relationship under cloudy and sunny conditions (Figure 8b). All these issues are worth further investigation with more observations in future studies.

4.3. Uncertainties and Implications of the Agricultural Based Continuous SIF Measurements

Ground-based continuous SIF measurements enable us to disentangle the confounding effects of factors such as plant growth stages and light conditions on the GPP:SIF and LUE:SIF_y relationships. This is even more important to the LUE:SIF_y relationship as its much smaller variation could be concealed by the confounding effects. In the current study, we observed the consistent positive SIF_y:APAR and negative LUE:APAR relationships under sunny conditions at both diurnal and seasonal scales. These patterns were strong under stable sunny conditions at early reproductive stage (Figures 5d and 5e and 7d and 7e)—the peak growing status with closed canopy and relatively stable chlorophyll content. Therefore, we believe that these patterns are robust and indicate the light responses of photosynthesis and SIF at the soybean field. These patterns also implicitly suggest the negative LUE:SIF_y relationship, providing an additional support to the weak directly derived LUE: SIF_y pattern (Figures 5f and 7f).

However, uncertainties related to the current field instrumentation require further attention and improvements in future studies. The different footprint sizes of GPP and SIF could impact the GPP:SIF relationship under instable light conditions. For example, during partly cloudy days, GPP might only change slightly due to the large footprint (hundreds of meters), while SIF measurements could fluctuate remarkably with clouds moving over its much smaller footprint area (1 m diameter in our system). These different responses to the changing light conditions might have caused the asymptotic GPP:SIF relationship we observed during cloudy days. In contrast, on stable sunny days, the changes in GPP and SIF were much less affected by the footprint difference. The SIF observation might be also impacted by the directionality (characterized by the bidirectional reflectance distribution function), although observing from the nadir partially reduces the effect. Multiangle observations of SIF could be helpful to characterize the uncertainties of directional effects (Liu et al., 2016). Additionally and importantly, the reabsorption of emitted SIF was not taken into account in this current study (Gitelson, Buschmann, & Lichtenthaler, 1998; Porcar-Castell et al., 2014), implying a potential gap between the observed SIF and the true SIF_y ($SIF = APAR \times SIF_y \times f_{esc}$, in which f_{esc} accounts for the fraction of SIF photons escaping from the canopy to be detected). It is challenging to measure the reabsorption in the

field, but modeling could help fill the gap (Dahn et al., 1992; Du et al., 2017), and this is an ongoing study area in the SIF community.

Our agricultural-based continuous measurements added a different scenario into the variety of the SIF_y: APAR and LUE:SIF_y relationships and provided new insights on the theoretical light partitioning framework of plant regulatory system (Schlau-Cohen & Berry, 2015). The variety of these relationships also suggests that despite the small contributions, LUE:SIF_y relationship may contain the information associated with some fundamental differences between ecosystems, in addition to the similar GPP:APAR and SIF:APAR relationships across various ecosystems. These fundamental differences in both physiology and canopy structure, such as the high photosynthetic capacity of soybean and the structural dynamics of sunlit and shaded leaves, could play important roles in interpreting the canopy-level GPP:SIF relationship but need to be tested by further comparisons in more ecosystems. It is also necessary to conduct measurements on more variables, such as LUE, SIF_y, and photosynthetic capacity of sunlit and shaded leaves under different light conditions, for a better understanding of physiological and structural effects on GPP:SIF relationship. Furthermore, the difference between observations and modeling results highlights the necessity of incorporating these observed patterns into fluorescence-related models (e.g., SCOPE model) for further tests to improve the model applicability in various ecosystems or under different conditions and provide the foundation to scale the SIF up at broader spatiotemporal scales for estimating GPP.

Acknowledgments

G.M. and K.G. acknowledge the support from the NASA New Investigator Award (NNX16AI56G) and support from the Institute for Sustainability, Energy, and Environment (iSEE) of University of Illinois at Urbana Champaign. K.G. and C.B. are also partially supported by the DOE TERRA-MEPP Project. X.Y. acknowledges the support from NASA Interdisciplinary Science Award (80NSSC17K0110). J.W. acknowledges the support from the United States Department of Energy contract DE-SC0012704 to Brookhaven National Laboratory. The authors also acknowledged the technical support from Timothy A. Mies and other staff in the Energy Farm of University of Illinois at Urbana-Champaign. Data of this study are available at https://doi.org/10.13012/B2IDB-1329706_V1.

References

Ac, A., Malenovsky, Z., Olejnickova, J., Galle, A., Rascher, U., & Mohammed, G. (2015). Meta-analysis assessing potential of steady-state chlorophyll fluorescence for remote sensing detection of plant water, temperature and nitrogen stress. *Remote Sensing of Environment*, *168*, 420–436. https://doi.org/10.1016/j.rse.2015.07.022

Badgley, G., Field, C. B., & Berry, J. A. (2017). Canopy near-infrared reflectance and terrestrial photosynthesis. *Science Advances*, *3*(3), e1602244. https://doi.org/10.1126/sciadv.1602244

Cogliati, S., Rossini, M., Julitta, T., Meroni, M., Schickling, A., Burkart, A., et al. (2015). Continuous and long-term measurements of reflectance and sun-induced chlorophyll fluorescence by using novel automated field spectroscopy systems. *Remote Sensing of Environment*, *164*, 270–281. https://doi.org/10.1016/j.rse.2015.03.027

Dahn, H. G., Gunther, K. P., & Ludeker, W. (1992). Characterisation of drought stress of maize and wheat canopies by means of spectral resolved laser induced fluorescence. EARSeL Advances in Remote Sensing.

Damm, A., Elber, J., Erler, A., Gioli, B., Hamdi, K., Hutjes, R., et al. (2010). Remote sensing of sun-induced fluorescence to improve modeling of diurnal courses of gross primary production (GPP). *Global Change Biology*, *16*(1), 171–186. https://doi.org/10.1111/j.1365-2486.%202009.01908.x

Damm, A., Guanter, L., Laurent, V. C. E., Schaepman, M. E., Schickling, A., & Rascher, U. (2014). FLD-based retrieval of sun-induced chlorophyll fluorescence from medium spectral resolution airborne spectroscopy data. *Remote Sensing of Environment*, *147*, 256–266. https://doi.org/10.1016/j.rse.2014.03.009

Damm, A., Guanter, L., Paul-Limoges, E., van der Tol, C., Hueni, A., Buchmann, N., et al. (2015). Far-red sun-induced chlorophyll fluorescence shows ecosystem-specific relationships to gross primary production: An assessment based on observational and modeling approaches. *Remote Sensing of Environment*, *166*, 91–105. https://doi.org/10.1016/j.rse.2015.06.004

Daumard, F., Champagne, S., Fournier, A., Goulas, Y., Ounis, A., Hanocq, J. F., & Moya, I. (2010). A field platform for continuous measurement of canopy fluorescence. *IEEE Transactions on Geoscience and Remote Sensing*, *48*(9), 3358–3368. https://doi.org/10.1109/TGRS.2010.2046420

Demmig, B., & Björkman, O. (1987). Comparison of the effect of excessive light on chlorophyll fluorescence (77K) and photon yield of O_2 evolution in leaves of higher plants. *Planta*, *171*(2), 171–184. https://doi.org/10.1007/BF00391092

Drolet, G., Wade, T., Nichol, C. J., MacLellan, C., Levula, J., Porcar-Castell, A., et al. (2014). A temperature-controlled spectrometer system for continuous and unattended measurements of canopy spectral radiance and reflectance. *International Journal of Remote Sensing*, *35*(5), 1769–1785. https://doi.org/10.1080/01431161.2014.882035

Du, S., Liu, L., Liu, X., & Hu, J. (2017). Response of canopy solar-induced chlorophyll fluorescence to the absorbed photosynthetically active radiation absorbed by chlorophyll. *Remote Sensing*, *9*(9). https://doi.org/10.3390/rs9090911

Fehr, W. R., Caviness, C. E., Burmood, D. T., & S., P. J. (1971). Stage of development descriptino for soybeans, Glycine max (L.) Merrill. *Crop Science*, *11*, 929–931. https://doi.org/10.2135/cropsci1971.0011183X001100060051x

Flexas, J., Escalona, J. M., Evain, S., Gulías, J., Moya, I., Osmond, C. B., & Medrano, H. (2002). Steady-state chlorophyll fluorescence (Fs) measurements as a tool to follow variations of net CO2 assimilation and stomatal conductance during water-stress in C3 plants. *European Space Agency, (Special Publication) ESA SP*, *527*, 26–29. https://doi.org/10.1034/j.1399-3054.2002.1140209.x

Fournier, A., Daumard, F., Champagne, S., Ounis, A., Goulas, Y., & Moya, I. (2012). Effect of canopy structure on sun-induced chlorophyll fluorescence. *ISPRS Journal of Photogrammetry and Remote Sensing*, *68*(1), 112–120. https://doi.org/10.1016/j.isprsjprs.2012.01.003

Frankenberg, C., Butz, A., & Toon, G. C. (2011). Disentangling chlorophyll fluorescence from atmospheric scattering effects in O2 A-band spectra of reflected Sun-light. *Geophysical Research Letters*, *38*, L03801. https://doi.org/10.1029/2010GL045896

Frankenberg, C., Fisher, J. B., Worden, J., Badgley, G., Saatchi, S. S., Lee, J. E., et al. (2011). New global observations of the terrestrial carbon cycle from GOSAT: Patterns of plant fluorescence with gross primary productivity. *Geophysical Research Letters*, *38*, L17706. https://doi.org/10.1029/2011GL048738

Gitelson, A., & Merzlyakb, N. (1994). Quantitative experiments estimation of chlorophyll-u using reflectance with autumn chestnut and maple leaves and spectra. *Journal of Photochemistry and Photobiology B: Biology*, *22*, 247–252.

Gitelson, A. A., Buschmann, C., & Lichtenthaler, H. K. (1998). Leaf chlorophyll fluorescence corrected for re-absorption by means of absorption and reflectance measurements. *Journal of Plant Physiology*, *152*(2–3), 283–296. https://doi.org/10.1016/S0176-1617(98)80143-0

Gitelson, A. A., Peng, Y., Arkebauer, T. J., & Suyker, A. E. (2015). Productivity, absorbed photosynthetically active radiation, and light use efficiency in crops: Implications for remote sensing of crop primary production. *Journal of Plant Physiology*, *177*, 100–109. https://doi.org/10.1016/j.jplph.2014.12.015

Gower, S. T., Kucharik, C. J., & Norman, J. M. (1999). Direct and indirect estimation of leaf area index, f(APAR), and net primary production of terrestrial ecosystems. *Remote Sensing of Environment*, *70*(1), 29–51. https://doi.org/10.1016/S0034-4257(99)00056-5

Grace, J., Nichol, C., Disney, M., Lewis, P., Quaife, T., & Bowyer, P. (2007). Can we measure terrestrial photosynthesis from space directly, using spectral reflectance and fluorescence? *Global Change Biology*, *13*(7), 1484–1497. https://doi.org/10.1111/j.1365-2486.2007.01352.x

Guan, K., Berry, J. A., Zhang, Y., Joiner, J., Guanter, L., Badgley, G., & Lobell, D. B. (2016). Improving the monitoring of crop productivity using spaceborne solar-induced fluorescence. *Global Change Biology*, *22*(2), 716–726. https://doi.org/10.1111/gcb.13136

Guanter, L., Zhang, Y., Jung, M., Joiner, J., Voigt, M., Berry, J. A., et al. (2014). Global and time-resolved monitoring of crop photosynthesis with chlorophyll fluorescence. *Proceedings of the National Academy of Sciences of the United States of America*, *111*(14), E1327–E1333. https://doi.org/10.1073/pnas.1320008111

Hilker, T., Coops, N. C., Wulder, M. A., Black, T. A., & Guy, R. D. (2008). The use of remote sensing in light use efficiency based models of gross primary production: A review of current status and future requirements. *Science of the Total Environment*, *404*(2–3), 411–423. https://doi.org/10.1016/j.scitotenv.%202007.11.007

Jenkins, J. P., Richardson, A. D., Braswell, B. H., Ollinger, S. V., Hollinger, D. Y., & Smith, M. L. (2007). Refining light-use efficiency calculations for a deciduous forest canopy using simultaneous tower-based carbon flux and radiometric measurements. *Agricultural and Forest Meteorology*, *143*(1–2), 64–79. https://doi.org/10.1016/j.agrformet.2006.11.008

Joiner, J., Guanter, L., Lindstrot, R., Voigt, M., Vasilkov, A. P., Middleton, E. M., et al. (2013). Global monitoring of terrestrial chlorophyll fluorescence from moderate spectral resolution near-infrared satellite measurements: Methodology, simulations, and application to GOME-2. *Atmospheric Measurement Techniques*, *6*(2), 2803–2823. https://doi.org/10.5194/amtd-6-3883-2013

Joiner, J., Yoshida, Y., Vasilkov, A. P., Yoshida, Y., Corp, L. A., & Middleton, E. M. (2011). First observations of global and seasonal terrestrial chlorophyll fluorescence from space. *Biogeosciences*, *8*(3), 637–651. https://doi.org/10.5194/bg-8-637-2011

Joo, E., Hussain, M. Z., Zeri, M., Masters, M. D., Miller, J. N., Gomez-casanovas, N., & Delucia, E. H. (2016). The influence of drought and heat stress on long-term carbon fluxes of bioenergy crops grown in the Midwestern USA. *Plant, Cell & Environment*, *39*, 1928–1940. https://doi.org/10.1111/pce.12751

Koller, D. (1990). Light-driven leaf movements. *Plant, Cell & Environment*, *13*(7), 615–632. https://doi.org/10.1111/j.1365-3040.1990.tb01079.x

Lemeur, R. (1973). A method for simulating the direct solar radiation regime in sunflower, jerusalem artichoke, corn and soybean canopies using actual stand structure data. *Agricultural Meteorology*, *12*(C), 229–247. https://doi.org/10.1016/0002-1571(73)90022-8

Liu, L., Guan, L., & Liu, X. (2017). Directly estimating diurnal changes in GPP for C3 and C4 crops using far-red sun-induced chlorophyll fluorescence. *Agricultural and Forest Meteorology*, *232*, 1–9. https://doi.org/10.1016/j.agrformet.2016.06.014

Liu, L., Liu, X., Wang, Z., & Zhang, B. (2016). Measurement and analysis of bidirectional SIF emissions in wheat canopies. *IEEE Transactions on Geoscience and Remote Sensing*, *54*(5), 2640–2651.

Louis, J., Ounis, A., Ducruet, J. M., Evain, S., Laurila, T., Thum, T., et al. (2005). Remote sensing of sunlight-induced chlorophyll fluorescence and reflectance of Scots pine in the boreal forest during spring recovery. *Remote Sensing of Environment*, *96*(1), 37–48. https://doi.org/10.1016/j.rse.2005.01.013

Malenovsky, Z., Mishra, K. B., Zemek, F., Rascher, U., & Nedbal, L. (2009). Scientific and technical challenges in remote sensing of plant canopy reflectance and fluorescence. *Journal of Experimental Botany*, *60*(11), 2987–3004. https://doi.org/10.1093/jxb/erp156

Meroni, M., Rossini, M., Guanter, L., Alonso, L., Rascher, U., Colombo, R., & Moreno, J. (2009). Remote sensing of solar-induced chlorophyll fluorescence: Review of methods and applications. *Remote Sensing of Environment*, *113*(10), 2037–2051. https://doi.org/10.1016/j.rse.2009.05.003

Moncrieff, J., Clement, R., Finnigan, J., & Meyers, T. (2004). Averaging, detrending, and filtering of eddy covariance time series. *Handbook of Micrometeorology*, *29*, 7–31. https://doi.org/10.1007/1-4020-2265-4_2

Moncrieff, J. B., Massheder, J. M., de Bruin, H., Elbers, J., Friborg, T., Heusinkveld, B., et al. (1997). A system to measure surface fluxes of momentum, sensible heat, water vapour and carbon dioxide. *Journal of Hydrology*, *188–189*, 589–611. https://doi.org/10.1016/S0022-1694(96)03194-0

Monteith, J. L. (1977). Climate and the efficiency of crop production in Britain. *Philosophical transactions of the Royal Society of London. Series B*, *281*, 277–294. https://doi.org/10.1098/rstb.2010.0098

Muller, P. (2001). Non-photochemical quenching. A response to excess light energy. *Plant Physiology*, *125*(4), 1558–1566. https://doi.org/10.1104/pp.125.4.1558

Papageorgiou, G. C., & Govindjee (Eds.) (2004). *Chlorophyll a fluorescence: A signature of photosynthesis*. Dordrecht, Netherlands: Kluwer Academic.

Papale, D., Reichstein, M., Aubinet, M., Canfora, E., Bernhofer, C., Kutsch, W., et al. (2006). Towards a standardized processing of Net Ecosystem Exchange measured with eddy covariance technique: Algorithms and uncertainty estimation. *Biogeosciences*, *3*(4), 571–583. https://doi.org/10.5194/bg-3-571-2006

Pearcy, R. W. (1990). Sunflecks and photosynthesis in plant canopies. *Annual Review of Plant Physiology and Plant Molecular Biology*, *41*, 421–453. https://doi.org/10.1016/0016-0032(53)91189-2

Perez-Priego, O., Guan, J., Rossini, M., Fava, F., Wutzler, T., Moreno, G., et al. (2015). Sun-induced chlorophyll fluorescence and photochemical reflectance index improve remote-sensing gross primary production estimates under varying nutrient availability in a typical Mediterranean savanna ecosystem. *Biogeosciences*, *12*(21), 6351–6367. https://doi.org/10.5194/bg-12-6351-2015

Pérez-Priego, O., Zarco-Tejada, P. J., Miller, J. R., Sepulcre-Cantó, G., & Fereres, E. (2005). Detection of water stress in orchard trees with a high-resolution spectrometer through chlorophyll fluorescence in-filling of the O2-A band. *IEEE Transactions on Geoscience and Remote Sensing*, *43*(12), 2860–2868. https://doi.org/10.1109/TGRS.2005.857906

Pinto, F., Damm, A., Schickling, A., Panigada, C., Cogliati, S., Muller-Linow, M., et al. (2016). Sun-induced chlorophyll fluorescence from high-resolution imaging spectroscopy data to quantify spatio-temporal patterns of photosynthetic function in crop canopies. *Plant, Cell and Environment*, *39*(7), 1500–1512. https://doi.org/10.1111/pce.12710

Porcar-Castell, A., Tyystjärvi, E., Atherton, J., Van Der Tol, C., Flexas, J., Pfündel, E. E., et al. (2014). Linking chlorophyll a fluorescence to photosynthesis for remote sensing applications: Mechanisms and challenges. *Journal of Experimental Botany*, *65*(15), 4065–4095. https://doi.org/10.1093/jxb/eru191

Rascher, U., Agati, G., Alonso, L., Cecchi, G., Champagne, S., Colombo, R., et al. (2009). CEFLES2: The remote sensing component to quantify photosynthetic efficiency from the leaf to the region by measuring sun-induced fluorescence in the oxygen absorption bands. *Biogeosciences*, *6*(1), 1181–1198. https://doi.org/10.5194/bgd-6-2217-2009

Rascher, U., Alonso, L., Burkart, A., Cilia, C., Cogliati, S., Colombo, R., et al. (2015). Sun-induced fluorescence—A new probe of photosynthesis: First maps from the imaging spectrometer HyPlant. *Global Change Biology*, *21*(12), 4673–4684. https://doi.org/10.1111/gcb.13017

Reichstein, M., Falge, E., Baldocchi, D., Papale, D., Aubinet, M., Berbigier, P., et al. (2005). On the separation of net ecosystem exchange into assimilation and ecosystem respiration: Review and improved algorithm. *Global Change Biology*, *11*(9), 1424–1439. https://doi.org/10.1111/j.1365-2486.%202005.001002.x

Rossini, M., Meroni, M., Migliavacca, M., Manca, G., Cogliati, S., Busetto, L., et al. (2010). High resolution field spectroscopy measurements for estimating gross ecosystem production in a rice field. *Agricultural and Forest Meteorology*, *150*(9), 1283–1296. https://doi.org/10.1016/j.agrformet.2010.05.011

Schlau-Cohen, G. S., & Berry, J. (2015). Photosynthetic fluorescence, from molecule to planet. *Physics Today*, *68*, 66–67.

Slattery, R. A., VanLoocke, A., Bernacchi, C. J., Zhu, X.-G., & Ort, D. R. (2017). Photosynthesis, light use efficiency, and yield of reduced-chlorophyll soybean mutants in field conditions. *Frontiers in Plant Science*, *8*, 1–19. https://doi.org/10.3389/fpls.2017.00549

Suyker, A. E., Verma, S. B., Burba, G. G., & Arkebauer, T. J. (2005). Gross primary production and ecosystem respiration of irrigated maize and irrigated soybean during a growing season. *Agricultural and Forest Meteorology*, *131*(3–4), 180–190. https://doi.org/10.1016/j.agrformet.2005.05.007

Tucker, C. J. (1979). Red and photographic infrared linear combinations for monitoring vegetation. *Remote Sensing of Environment*, *8*(2), 127–150. https://doi.org/10.1016/0034-4257(79)90013-0

Turner, D. P., Urbanski, S., Bremer, D., Wofsy, S. C., Meyers, T., Gower, S. T., & Gregory, M. (2003). A cross-biome comparison of daily light use effciency for gross primary production. *Global Change Biology*, *9*, 383–395. https://doi.org/10.1046/j.1365-2486.2003.00573.x

Van Der Tol, C., Berry, J. A., Campbell, P. K. E., & Rascher, U. (2014). Models of fluorescence and photosynthesis for interpreting measurements of solar-induced chlorophyll fluorescence. *Journal of Geophysical Research: Biogeosciences*, *119*, 2312–2327. https://doi.org/10.1002/2014JG002713

Van Der Tol, C., Rossini, M., Rascher, U., Verhoef, W., & Mohammed, G. (2016). A model and measurement comparison of diurnal cycles of Sun induced chlorophyll fluorescence of crops. *Remote Sensing of Environment*, *186*(iii), 1–13. https://doi.org/10.1016/j.rse.2016.09.021

Van Der Tol, C., Verhoef, W., & Rosema, A. (2009). A model for chlorophyll fluorescence and photosynthesis at leaf scale. *Agricultural and Forest Meteorology*, *149*, 96–105. https://doi:10.1016/j.agroformet.2008.07.007

Verma, M., Schimel, D., Evans, B., Frankenberg, C., Beringer, J., Drewry, D. T., et al. (2017). Effect of environmental conditions on the relationship between solar induced fluorescence and gross primary productivity at an OzFlux grassland site. *Journal of Geophysical Research: Biogeosciences*, *122*, 716–733. https://doi.org/10.1002/2016JG003580

Viña, A., & Gitelson, A. A. (2005). New developments in the remote estimation of the fraction of absorbed photosynthetically active radiation in crops. *Geophysical Research Letters*, *32*, L17403. https://doi.org/10.1029/2005GL023647

Viña, A., Gitelson, A. A., Nguy-Robertson, A. L., & Peng, Y. (2011). Comparison of different vegetation indices for the remote assessment of green leaf area index of crops. *Remote Sensing of Environment*, *115*(12), 3468–3478. https://doi.org/10.1016/j.rse.2011.08.010

Webb, E. K., Pearman, G. I., & Leuning, R. (1980). Correction of flux measurements for density effects due to heat and water vapour transfer. *Quarterly Journal of the Royal Meteorological Society*, *106*, 85–100. https://doi.org/10.1002/qj.49710644707

Weiss, A., & Norman, J. M. (1985). Partitioning solar radiation into direct and diffuse, visible and near-infrared components. *Agricultural and Forest Meteorology*, *34*(7441), 205–213.

Wood, J. D., Griffis, T. J., Baker, J. M., Frankenberg, C., Verma, M., & Yuen, K. (2016). Multi-scale analyses reveal robust relationships between gross primary production and solar induced fluorescence. *Geophysical Research Letters*, *44*, 533–541. https://doi.org/10.1002/2016GL070775

Yang, X., Tang, J., Mustard, J. F., Lee, J., & Rossini, M. (2015). Solar-induced chlorophyll fluorescence that correlates with canopy photosynthesis on diurnal and seasonal scales in a temperate deciduous forest. *Geophysical Research Letters*, *42*, 2977–2987. https://doi.org/10.1002/2015GL063201

Zarco-Tejada, P. J., Berni, J. A. J., Suarez, L., Sepulcre-Cantó, G., Morales, F., & Miller, J. R. (2009). Imaging chlorophyll fluorescence from an airborne narrow-band multispectral camera for vegetation stress detection. *Remote Sensing of Environment*, *113*, 1262–1275.

Zarco-Tejada, P. J., González-Dugo, V., & Berni, J. A. J. (2012). Fluorescence, temperature and narrow-band indices acquired from a UAV platform for water stress detection using a micro-hyperspectral imager and a thermal camera. *Remote Sensing of Environment*, *117*, 322–337. https://doi.org/10.1016/j.rse.2011.10.007

Zarco-Tejada, P. J., Morales, A., Testi, L., & Villalobos, F. J. (2013). Spatio-temporal patterns of chlorophyll fluorescence and physiological and structural indices acquired from hyperspectral imagery as compared with carbon fluxes measured with eddy covariance. *Remote Sensing of Environment*, *133*, 102–115. https://doi.org/10.1016/j.rse.2013.02.003

Zeri, M., Anderson-teixeira, K., Hickman, G., Masters, M., Delucia, E., & Bernacchi, C. J. (2011). Agriculture, ecosystems and environment carbon exchange by establishing biofuel crops in Central Illinois. *Agriculture, Ecosystems and Environment*, *144*(1), 319–329. https://doi.org/10.1016/j.agee.2011.09.006

Zhang, Y., Guanter, L., Berry, J. A., Joiner, J., van der Tol, C., Huete, A., et al. (2014). Estimation of vegetation photosynthetic capacity from space-based measurements of chlorophyll fluorescence for terrestrial biosphere models. *Global Change Biology*, *20*(12), 3727–3742. https://doi.org/10.1111/gcb.12664

Zhang, Y., Guanter, L., Berry, J. A., Van Der Tol, C., & Yang, X. (2016). Model-based analysis of the relationship between sun-induced chlorophyll fl uorescence and gross primary production for remote sensing applications. *Remote Sensing of Environment*, *187*, 145–155. https://doi.org/10.1016/j.rse.2016.10.016